

# Locomotion of a Snake-like Robot Controlled by the Bidirectional Cyclic Inhibitory CPG Model\*

Zhenli Lu<sup>1,3,4</sup> Shugen Ma<sup>1,2</sup> Bin Li<sup>1</sup> Yuechao Wang<sup>1</sup>

<sup>1</sup>Robotics Laboratory, Shenyang Institute of Automation, CAS, 114 Nanta Street, Shenyang, 110015 P. R. China

<sup>2</sup>Organization for Promotion of the COE Program, Ritsumeikan University, Shiga-Kan, 525-8577 Japan

<sup>3</sup>Graduate School of the Chinese Academy of Sciences, Beijing, 100039 P. R. China

<sup>4</sup>Shenyang Ligong University, Shenyang, 110168 P. R. China

luzhl@sia.ac.cn shugen@fc.ritsumei.ac.jp libin@sia.ac.cn ycwang@sia.ac.cn

**Abstract**—With slim and legless body, particular ball articulation and rhythmic locomotion, a nature snake adapted itself to many terrains under the control of neuron system. Based on analyzing the locomotion mechanism, the main functional features of the motor system in snakes are specified in detail. Furthermore, a bidirectional cyclic inhibitory CPG model is firstly applied to imitate the pattern generation for the locomotion control of the snake-like robot, and its characteristic is discussed particularly for the generation of different kinds rhythmic locomotion. Besides, we introduce the neuron network organized by the bidirectional cyclic inhibitory CPGs connected in line with unilateral excitation to switch automatically locomotion pattern of a snake-like robot under different command from high level neuron, and present the necessary condition for the CPG neuron network to sustain a rhythmic output. The validity for the generation of different kinds of rhythmic locomotion modes by the CPG network are verified by the dynamic simulations and experiments. This research provided a new method to model the generation mechanism of the rhythmic pattern of the snake.

**Index Terms**—Snake-like robot. Bidirectional cyclic inhibition. Central pattern generator (CPG). Stability analysis. Locomotion control.

## I. INTRODUCTION

Snakes form one of the world's most successful groups of animals, as shown in Fig.1a. They live on every continent but Antarctica and number approximately 3,000 different species. They can be found not only on or under the ground, but also in lakes, rivers, and oceans. Snakes can have between 130-500 vertebrae in their cylindrical, legless body, as shown in Fig.1b. The vertebrae articulate with the usual cup and ball articulation, with the almost hemispherical condyle on the back of the vertebrae. The neural arch is provided with additional articular surfaces in the form of pre-zygapophyses and post-zygapophyses [1].

Snakes perform many kinds of rhythmic movements adapted to their environment. Locomotive motions such as locomotion of serpentine locomotion, side winding locomotion, concertina locomotion etc. are typical examples of oscillatory activities of the snake. The key component of

the motor system is the Central Pattern Generator (CPG), a neural circuit that can produce a rhythm motor pattern with no need for sensory feedback or descending control. It is mainly located in the spinal cord of vertebrates or in relevant ganglia in invertebrates [2]. To explain the mechanism of such autonomic oscillatory activities, various models of CPG have been suggested [3]. In all the models, neurons are connected such that one neuron's excitation suppresses the other neurons' excitations. Reiss (1962) showed that a pair of reciprocally inhibiting neurons with fatigue can produce alternate bursts of firing [4]. Kling and Szekely (1968) investigated rhythmic activities of circular networks with cyclic inhibitions [5]. Matsuoka (1985) gave mathematical condition for mutual inhibition networks represented by a continuous-variable neuron model to generate oscillations [6].

Snake-like robot that behaves to imitate the shape and locomotion of the snake is studied all over the world [7]. Ma's group (2004) adopted mutual inhibitory CPG to construct a control system for the creeping locomotion of a snake-like robot [8]. But it is only suitable for 2D (2-dimensional) locomotion control. Ma's group (2005) also proposed a cyclic inhibitory CPG for the 3D (3-dimensional) locomotion control of a snake-like robot [9], which can also realize creeping locomotion by cancelling the pitch joint controlling signal [10], [11]. However a rhythmic pattern can not be switched to another pattern by temporarily changing the stimulus pattern in all above CPG control system for the locomotion of the snake-like robot. It is not resembled the mechanism of nature snakes.

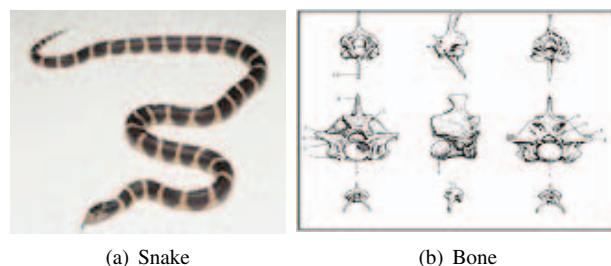


Fig. 1. Snake and its bone structure

In order to solve this problem, we proposed a bidirectional cyclic inhibitory CPG for the locomotion control and pattern

\*This work is supported by the National Science Foundation of China under Grant 60375029, the National Hi-tech Research and Development Plan (No.2001AA422360), and partially supported by the JSPS, Grants-in-Aid (No.15360129).

switch of a snake-like robot to imitate the mechanism of nature snakes. The CPG is a kind of relaxation oscillator, requiring the adaptation for rhythm generation.

The reminder of this paper is organized as follows: In section II, we specify four kinds of typical rhythm locomotion of snakes and their rhythm pattern generation mechanism. The structure of the bidirectional cyclic inhibitory CPG model is proposed in section III. In section IV, a detailed analysis about the CPG is presented. The controller constructed by the bidirectional cyclic inhibitory CPGs for the rhythmic pattern control to the locomotion of the snake-like robot is addressed in section V. Moreover, the dynamic simulations and experiments are carried out to verify the proposed architecture for the robot to realize different locomotion in section VI. Finally, the conclusions are discussed in section VII.

## II. TYPICAL LOCOMOTION OF SNAKES AND GENERATION MECHANISM

Four quite different types of rhythmic locomotion are used by snakes, as shown in Fig.2.

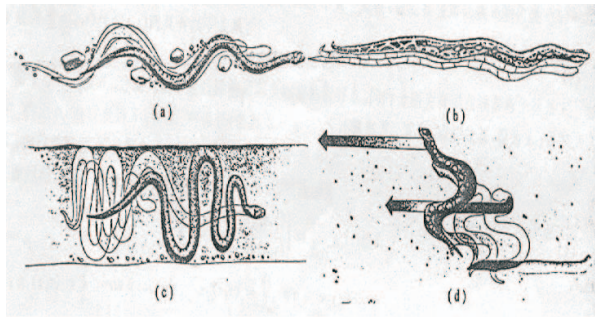


Fig. 2. Typical locomotion types of snakes: (a) serpentine locomotion, (b) rectilinear locomotion, (c) concertina locomotion, (d) side winding locomotion

In serpentine locomotion, the snake pushes against the ground on the back side of each curve or undulation and flows smoothly forwards. It is the result of the hemispherical condyles on the back of the vertebrae swayed only in the horizontal plan. In rectilinear locomotion, the skin of the ventral surface is moved forwards and backwards by strong muscles, and the broad belly scales grip the ground, moving the snake forwards in a straight line. It is used only by the heavier-bodied snakes, so we do not consider it here. In concertina locomotion, the body is alternately stretched out and pulled together as the snake moves from one anchor point to another. It is used in crossing smooth surfaces and in climbing. It is the result of the hemispherical condyles on the back of the vertebrae swayed only in the vertical plan. Several desert-dwelling species use sidewinding to move on loose sand. In this method the snake throws its body sideways along the ground in a looping motion. It is the result of the hemispherical condyles on the back of the vertebrae swayed in 3D plan. Actually the ribs do not move forwards and backwards in any of the four types of movements. Muscles are versatile motors. They can pull against each other and against

their tendons in complex ways [12]. The great importance of the CPG lies in the fact that central pattern generators of rhythms have been demonstrated in all animals to account for rhythmic movements (defined by Shepherd [13]). Based on the above theory, we proposed the mechanism of the rhythm locomotion of snakes is that a set of muscles located among the vertebrae received the stimulus of CPG to generate the rotation of the hemispherical condyle. Its functional subdivision is familiar with other vertebrate, as shown in Fig.3. In the subsystem, the CPG can generate the corresponding rhythmic pattern for the serpentine locomotion, concertina locomotion and side winding locomotion. Feedback from the Central Pattern Generator directed to the higher level control neurons, the feedback from the effector organs to the CPG, and the feedback from the environment to either the CPG or to high level neuron. The feedback signals modify the locomotion pattern and are fundamental to achieve good performance by the whole control system in real environment. Besides eliciting the motor system pattern, the higher control neurons are responsible for important decisions such as the choice of the right locomotion pattern or escape reaction. Here we do not consider the feedback, only study on the CPG mechanism under the high level neuron control for the rhythmic pattern generation of the three typical locomotion of the snake, which is verify by the simulations and experiments on the snake-like robot.

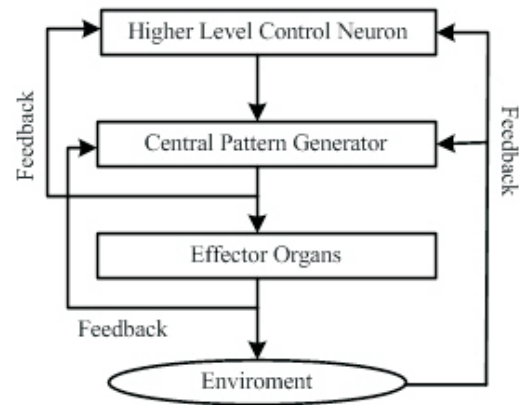


Fig. 3. Main functional features of motor system

## III. BIDIRECTIONAL CYCLIC INHIBITORY CPG

Using a reciprocal inhibition among three neuron, and give all synaptic weights equal values, we constructed a bidirectional cyclic inhibitory CPG model which is a completely symmetric structure in terms of graph theory. This bidirectional cyclic inhibitory CPG is composed of  $n_y$  (yaw neuron),  $n_p$  (pitch neuron), and  $n_m$  (modulate neuron). Here we adopted a combined joint whose rotational axis connected perpendicularly to imitate the locomotion of the hemispherical condyle in snakes. The Structure of the CPG and its control relation with the combined joint is shown in Fig.4. We utilize Matsuoka's neuron model [14] to specify the CPG, as shown

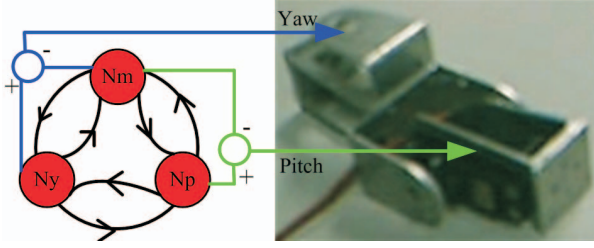


Fig. 4. CPG and its control relation with combined joint

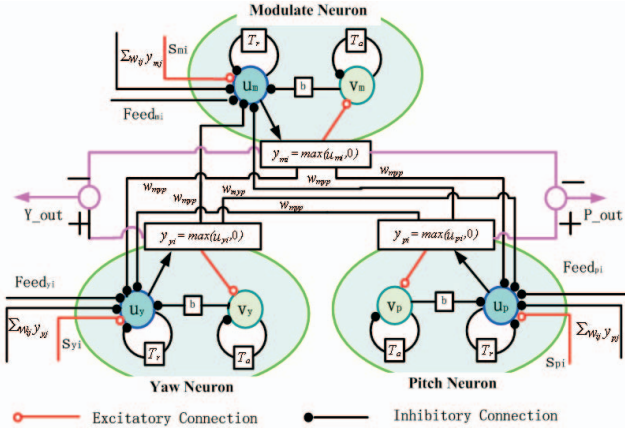


Fig. 5. Bidirectional cyclic inhibitory CPG model

in Fig.5. The dynamics of the bidirectional cyclic inhibitory CPG is described by the following equations:

$$T_r \dot{u}_{\{y,p,m\},i} = -u_{\{y,p,m\},i} - w_{\{y,p,m\},i} y_{\{p,m,y\},i} - w_{\{y,p,m\},i} y_{\{m,y,p\},i} - b v_{\{y,p,m\},i} + s_{\{y,p,m\},i} + \sum_{j=1}^n w_{ij} y_{\{y,p,m\},j} + Feed_{\{y,p,m\},i} \quad (1)$$

$$T_a \dot{v}_{\{y,p,m\},i} = -v_{\{y,p,m\},i} + y_{\{y,p,m\},i} \quad (2)$$

$$y_{\{y,p,m\},i} = \max(0, u_{\{y,p,m\},i}) \quad (3)$$

$$y_{yaw,i} = y_{yi} - y_{mi} \quad (4)$$

$$y_{pitch,i} = y_{pi} - y_{mi} \quad (5)$$

where  $u_{\{y,p,m\},i}$  describes respectively membrane potentials of  $n_y$ ,  $n_p$  or  $n_m$  of  $i$ -th CPG;  $v_{\{y,p,m\},i}$  describes respectively adaptation of  $n_y$ ,  $n_p$  or  $n_m$  of  $i$ -th CPG;  $T_r$  shows respectively time constants of membrane potential of  $n_y$ ,  $n_p$  or  $n_m$  of  $i$ -th CPG;  $T_a$  shows respectively time constants of adaptation of  $n_y$ ,  $n_p$  or  $n_m$  of  $i$ -th CPG;  $w_{\{y,p,m\},i}$  shows respectively connection weight among  $n_y$ ,  $n_p$  or  $n_m$  of  $i$ -th CPG, here we set it as a constant  $w_{ypm}$ ;  $b$  gives respectively connection weight inner  $n_y$ ,  $n_p$  or  $n_m$  of  $i$ -th CPG;  $w_{ij}$  is connection weight between  $i$ -th and  $j$ -th CPG;  $s_{\{y,p,m\},i}$  are constant, positive input, each of which is the summation of all inputs to  $n_y$ ,  $n_p$  or  $n_m$  by the weight of synaptic conjunction, excepting the output of the neuron in the  $i$ -th CPG;  $y_{\{y,p,m\},i}$  are outputs of  $n_y$ ,  $n_p$  or  $n_m$  of  $i$ -th CPG;  $y_{\{yaw,pitch\},i}$  are CPG control signal of yaw or pitch joint of  $i$ -th combined joint;  $Feed_{\{y,p,m\},i}$  are feedback of  $n_y$ ,  $n_p$  or  $n_m$  of  $i$ -th CPG.

#### IV. ANALYSIS OF MECHANISM FOR RHYTHM GENERATION

Before analyzing the stability of the stationary states we specify a theorem on the existence, uniqueness and boundedness of the solution of (1), (2).

**Theorem 1.** A solution of Eq.(1), (2) exists uniquely for any initial state and is bounded for  $t \geq 0$ .

*proof.* The existence and the uniqueness of the solution of Eq.(1), (2) can be proved by checking Lipschitz's condition. Expressing Eq.(1), (2) in the following form:  $\dot{x} = f(t, x)$ . Here, we do not consider the stimulus from other CPG,  $w_{ij} = 0$ ; and no feedback signal,  $Feed_{\{y,p,m\},i} = 0$ .

$$f(t, u_{\{y,p,m\},i}) = \frac{1}{T_r} (-u_{\{y,p,m\},i} - w_{ypm} u_{\{p,m,y\},i} - w_{ypm} u_{\{m,y,p\},i} + s_{\{y,p,m\},i} - b v_{\{y,p,m\},i}) \quad (6)$$

$$f(t, v_{\{y,p,m\},i}) = \frac{1}{T_a} (-v_{\{y,p,m\},i} + u_{\{y,p,m\},i}) \quad (7)$$

Since we assume:  $|u_{\{y,p,m\},i} - u'_{\{y,p,m\},i}| \leq |u_{\{y,p,m\},i} - u'_{\{p,m,y\},i}| \leq |u_{\{y,p,m\},i} - u'_{\{m,y,p\},i}| \leq \rho_1$ ,  $|v_{\{y,p,m\},i} - v'_{\{y,p,m\},i}| \leq \rho_2$ ,  $|s_{\{y,p,m\},i} - s'_{\{y,p,m\},i}| \leq \rho_3$ , for every  $|t - t'| \leq \rho$ .

We get:

$$|f(t, u_{\{y,p,m\},i}) - f(t, u'_{\{y,p,m\},i})| \leq \left| \frac{2w_{ypm}+1}{T_r} + \frac{b\rho_2-\rho_3}{T_r\rho_1} \right| (u_{\{y,p,m\},i} - u'_{\{y,p,m\},i}) \quad (8)$$

$$|f(t, v_{\{y,p,m\},i}) - f(t, v'_{\{y,p,m\},i})| \leq \left| \frac{\rho_1-\rho_2}{\rho_2 T_a} \right| (v_{\{y,p,m\},i} - v'_{\{y,p,m\},i}) \quad (9)$$

Thus,

$$|f(t, X) - f(t, X')| \leq L |X - X'| \quad (10)$$

Here,  $L = \max(|\frac{2w_{ypm}+1}{T_r} + \frac{b\rho_2-\rho_3}{T_r\rho_1}|, |\frac{\rho_1-\rho_2}{\rho_2 T_a}|)$ . Thus Eq.(1),(2) satisfied the Lipschitz's condition. Q.E.D.

To prove the boundedness, solve Eq.(2) with respect to  $v_{\{y,p,m\},i}(t)$ :

$$v_{\{y,p,m\},i}(t) = v_{\{y,p,m\},i}(0) e^{-\frac{t}{T_a}} + \frac{1}{T_a} e^{-\frac{t}{T_a}} \int_0^t g(u_{\{y,p,m\},j}(x)) e^{\frac{x}{T_a}} dx \quad (11)$$

Since  $g(u_{\{y,p,m\},j}(x))$  is nonnegative,

$$v_{\{y,p,m\},i}(t) \geq -|v_{\{y,p,m\},i}(0)|, t \geq 0 \quad (12)$$

Solving Eq.(1) with respect to  $u_{\{y,p,m\},i}(t)$ , we obtain

$$u_{\{y,p,m\},i}(t) = u_{\{y,p,m\},i}(0) e^{-\frac{t}{T_r}} + s_{\{y,p,m\},i} (\frac{1}{T_r} - \frac{1}{T_r} e^{-\frac{t}{T_r}}) - \frac{w_{ypm}}{T_r} \int_0^t g(u_{\{p,m,y\},j}(x)) e^{\frac{x}{T_r}} dx - \frac{w_{ypm}}{T_r} \int_0^t g(u_{\{m,y,p\},j}(x)) e^{\frac{x}{T_r}} dx - \frac{b}{T_r} \int_0^t v_{\{y,p,m\},j}(x) e^{\frac{x}{T_r}} dx \quad (13)$$

Applying (12) to (13), we get

$$u_{\{y,p,m\},i}(t) \leq |u_{\{y,p,m\},i}(0)| + |\frac{1}{T_r} s_{\{y,p,m\},i}(0)| + |\frac{b}{T_r} v_{\{y,p,m\},i}(0)| \quad (14)$$



Applying (14) to (11) gives similarly

$$v_{\{y,p,m\},i}(t) \leq |v_{\{y,p,m\},i}(0)| + \left| \frac{1}{T_a} \right| (|u_{\{y,p,m\},i}(0)| + \left| \frac{1}{T_r} s_{\{y,p,m\},i}(0) \right| + \left| \frac{b}{T_r} v_{\{y,p,m\},i}(0) \right|). \quad (15)$$

Applying (14) and (15) once again to (13), we obtain

$$\begin{aligned} u_{\{y,p,m\},i}(t) \geq & -|u_{\{y,p,m\},i}(0)| - \left| \frac{1}{T_r} s_{\{y,p,m\},i}(0) \right| \\ & - \left| \frac{w_{ypm}}{T_r} \right| (|u_{\{p,m,y\},i}(0)| + \left| \frac{1}{T_r} s_{\{p,m,y\},i}(0) \right| \\ & + \left| \frac{b}{T_r} v_{\{p,m,y\},i}(0) \right|) \\ & - \left| \frac{w_{ypm}}{T_r} \right| (|u_{\{m,y,p\},i}(0)| + \left| \frac{1}{T_r} s_{\{m,y,p\},i}(0) \right| \\ & + \left| \frac{b}{T_r} v_{\{m,y,p\},i}(0) \right|) \\ & - \left| \frac{b}{T_r} \right| \{ |v_{\{y,p,m\},i}(0)| + \left| \frac{1}{T_a} \right| (|u_{\{y,p,m\},i}(0)| \\ & + \left| \frac{1}{T_r} s_{\{y,p,m\},i}(0) \right| + \left| \frac{b}{T_r} v_{\{y,p,m\},i}(0) \right|) \}. \end{aligned} \quad (16)$$

From (12), (14), (15), and (16) we can conclude that any solution of Eq.(1), (2) is bounded for  $t \geq 0$ . Q.E.D.

Thus, a solution of Eq.(1), (2) exists uniquely for any initial state and is bounded for  $t \geq 0$ .

Theorem 2. Equation (1), (2) has at least one stationary solution.

Proof. Define a bounded, convex region  $D$  in the  $3n$ -dimensional Euclidean space  $R^{3n}$  by  $D = (0 \leq y_{\{y,p,m\},i} \leq s_{\{y,p,m\},i}; i = 1, \dots, n)$ .

Since  $0 \leq g(\frac{1}{T_r}(-w_{ypm}by_{\{p,m,y\},i}^0 - w_{ypm}by_{\{p,m,y\},i}^0 + s_{\{y,p,m\},i} - by_{\{y,p,m\},i}^0)) \leq s_{\{y,p,m\},i}$ , for arbitrary  $y_{\{y,p,m\},i}^0 (i = 1, \dots, n)$ ,  $F$  is a continuous, contractive mapping from  $D$  into  $D$ . According to Brower's fixed point theorem there must be a fixed point of  $F$  and it is a stationary solution of Eq. (1), (2). Q.E.D.

Stability of a stationary solution will be found by investigating the differential equation which is obtained by linearizing Eq.(1), (2) in the vicinity of the stationary solution. If the origin of Eq. (1), (2) is unstable for every stable stationary state or Eq. (1), (2) has no stable stationary state, then every solution (other than the unstable stationary states) must be oscillatory (not necessarily periodic) due to the boundedness of the solution. According to the theorem in reference [6], we proposed a condition for the CPG network to sustain a stable oscillation:

$$\frac{w_{ypm}}{1+b} \leq \min \left( \frac{\sin_{\{y,p,m\},i}}{\sin_{\{p,m,y\},i}}, \frac{\sin_{\{y,p,m\},i}}{\sin_{\{m,y,p\},i}}, \frac{\sin_{\{p,m,y\},i}}{\sin_{\{m,y,p\},i}} \right), \quad (17)$$

$$w_{ypm} > 1 + \frac{T_r}{T_a}. \quad (18)$$

Here  $\sin_{\{y,p,m\},i}$  are the sum of the input to  $i$ -th  $n_{\{y,p,m\}}$ .

The rhythmic output of the neurons inner an isolated CPG under single neuron first fired is [No1, No2, No2], as shown in Fig.6. The corresponding rhythmic output of the CPG is shown in Fig.7.

An interesting feature of this CPG is that it can generate the following rhythm patterns under different initial condition: Case 1:  $n_y(\text{No1}) > (n_p(\text{No2}) = n_m(\text{No2})) > n_y(\text{No1}) > (n_p(\text{No2}) = n_m(\text{No2})) \dots$ , (only  $n_y$  is fired first), and the output of the CPG is  $y_{yaw}(\text{Co1}), y_{pitch}(\text{Co2})$ . This is the rhythm pattern for the combined joint rotating in horizontal plan.

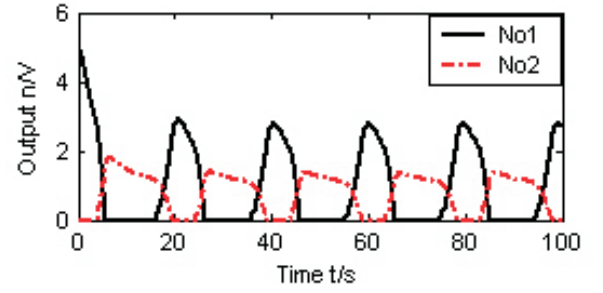


Fig. 6. Neuron Output in a CPG (No1: output of first fired neuron; No2: output of two unfired neurons)

Case 2:  $n_p(\text{No1}) > (n_m(\text{No2}) = n_y(\text{No2})) > n_p(\text{No1}) > (n_m(\text{No2}) = n_y(\text{No2})) \dots$ , (only  $n_p$  is fired first), and the output of the CPG is  $y_{yaw}(\text{Co2}), y_{pitch}(\text{Co1})$ . This is the rhythm pattern for the combined joint rotating in vertical plan.

Case 3:  $n_m(\text{No1}) > (n_y(\text{No2}) = n_p(\text{No2})) > n_m(\text{No1}) > (n_y(\text{No2}) = n_p(\text{No2})) \dots$ , (only  $n_m$  is fired first), and the output of the CPG is  $y_{yaw}(\text{Co1}), y_{pitch}(\text{Co1})$ . This is the rhythm pattern for the combined joint rotating in 3D plan. ( $>$  indicate the time order of firing neurons,  $=$  indicate the same rhythm of firing neurons).

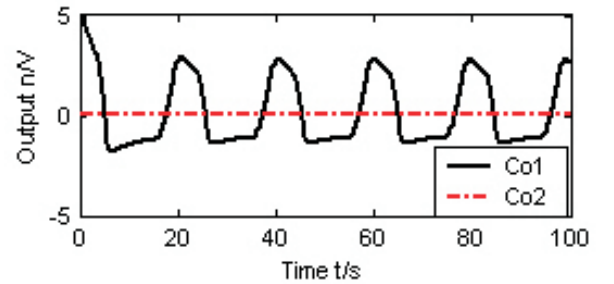


Fig. 7. CPG output (Co1: CPG output by first fired and unfired neurons; Co2: CPG output by two unfired neurons)

## V. CONSTRUCTION OF CPG CONTROL SYSTEM FOR SNAKE-LIKE ROBOT

Snake epaxial muscle-tendon networks are among the longest multi-joint muscle systems. The complex interconnections and large cross-sectional areas suggest that the epaxial muscles are major axial flexors. These muscles mainly produce broad bends in long segments of the body, but they are also active in sharper bending during constriction. In behaviors that involve undulatory movements, the long muscle-tendon networks pull on each other and on vertebral joints in complex ways that appear to enhance strength and reduce energy use [12]. As the first step of our research, the bidirectional cyclic inhibitory CPGs mentioned above are connected in a series by the single excitatory synapse from head to tail, to construct the control system architecture of the snake-like robot, as shown in Fig.8.

The mechanism of the CPG network is the first CPG receive the high level control signal to generate the corre-

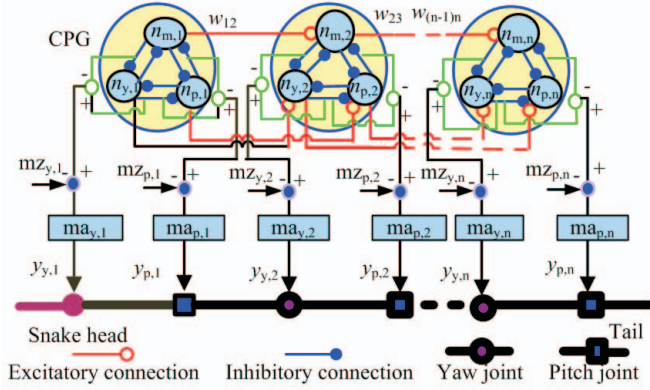


Fig. 8. CPG control system of the snake-like robot

sponding rhythm pattern. The neurons in the following CPGs are fired by the synapse connection from the corresponding neuron of its front CPG. The pattern of the rhythm is thus propagating from the head to the tail with a specific physic difference. As a result, the corresponding locomotion of the snake-like robot is achieved. Here we use the parameter  $ma_{\{y,z\},i}$  to modulate signal of the  $i$ -th combined joint's amplitude, and  $mz_{\{y,z\},i}$  to modulate the phase of the signal to the  $i$ -th combined joint,  $i = 1, \dots, 4$ .

## VI. SIMULATIONS AND EXPERIMENTS

According to the parameters of "Perambulator", we adopted ADAMS software to construct a 3D dynamic model of the snake-like robot (for details see reference [9]). Based on the theory in reference [2] that the high level neuron just sends rhythm selection command, the CPG network can generate the corresponding rhythm pattern under it automatically, we use the CPG network to generate different rhythm pattern for the locomotion control of serpentine locomotion (only  $n_{y,1}$  first fired), concertina locomotion (only  $n_{p,1}$  first fired) and side winding locomotion (only  $n_{m,1}$  first fired).

1) *Parameter Setting*: According to condition (17), (18) and reference [14], we specify the parameters of the CPG network, as shown in table 1. The output of the neurons in CPG network is shown as following: CPG<sub>1</sub>: [sno1,sno2,sno2], CPG<sub>2</sub>: [sno3,sno4,sno4], CPG<sub>3</sub>: [sno5,sno6,sno6], CPG<sub>4</sub>: [sno7,sno8,sno8], as shown in Fig.9. The output of the CPGs is shown in Fig.10. From Fig.9 we know, under the signal neuron first fired condition, the CPG output from first fired neuron and the other neuron is a rhythm pattern. The CPG output from the two unfired in the first time is zero in the first CPG. And the following CPG have the same rhythm pattern out put, just have a specific difference.

2) *Simulations*: In the dynamic simulator, the contact between the robot and the environment is defined as a coulomb friction. The coefficient of the static friction is 0.3, and the coefficient of the dynamic friction is 0.1. The output of the CPG neuron network was adopted as the input of the 3D dynamic model of the snake-like robot.

TABLE I  
PARAMETERS OF "PERAMBULATOR"

Positive input $s_{0,\{y,p,m\},i}/V$ ( $i = 1, \dots, 4$ )	5
Time constant $T_r/s$	1
Time constant $T_a/s$	12
Connection weight inner a CPG $w_{\{y,p,m\},i}$ ( $i = 1, \dots, 4$ )	1.5
Connection weight among CPGs $w_{ij}$ ( $j = i + 1; i = 1, \dots, 4$ )	0.1
Connection weight inner a neuron $b$	2.5

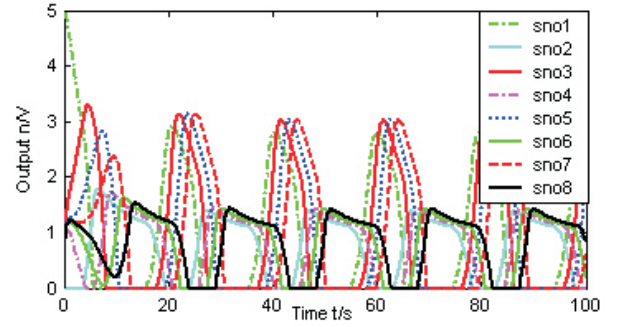


Fig. 9. Neurons' output of the CPG network

Under the high level command to initial fire the  $[n_{y,1}, n_{p,1}, n_{m,1}]$ , other CPG is unfired at the beginning to the CPG network, ( $i = 1, \dots, 4$ ). Case[100]:  $[n_{y,i}, n_{p,i}, n_{m,i}]$  is  $\{[sno1, sno2, sno2], [sno3, sno4, sno4], [sno5, sno6, sno6], [sno7, sno8, sno8]\}$ , the output of  $[y_{yaw,i}, y_{pitch,i}]$  is  $\{[sco1, sco5], [sco2, sco5], [sco3, sco5], [sco4, sco5]\}$ . It is the rhythm pattern for the locomotion control of serpentine locomotion. Case [010]:  $[n_{y,i}, n_{p,i}, n_{m,i}]$  is  $\{[sno2, sno1, sno2], [sno4, sno3, sno4], [sno6, sno5, sno6], [sno8, sno7, sno8]\}$ , the output of  $[y_{yaw,i}, y_{pitch,i}]$  is  $\{[sco5, sno1], [sco5, sco2], [sco5, sco3], [sco5, sco4]\}$ . It is the rhythm pattern for the locomotion control of concertina locomotion. Case [001]:  $[n_{y,i}, n_{p,i}, n_{m,i}]$  is  $\{[sno2, sno2, sno1], [sno4, sno4, sno3], [sno6, sno6, sno5], [sno8, sno8, sno7]\}$ , the output of  $[y_{yaw,i}, y_{pitch,i}]$  is  $\{[sco1, sco1], [sco2, sco2], [sco3, sco3], [sco4, sco4]\}$ . It is the rhythm pattern for the locomotion control of side winding locomotion.

Here 1 indicates fired neuron; 0 : indicate unfired neuron. In order to verify the above result, we sent  $ma_{\{y,p,m\},i} = 0.3$ ,  $mz_{\{y,p,m\},i} = 1, i = 1, \dots, 4$ . We adopted the data shown in

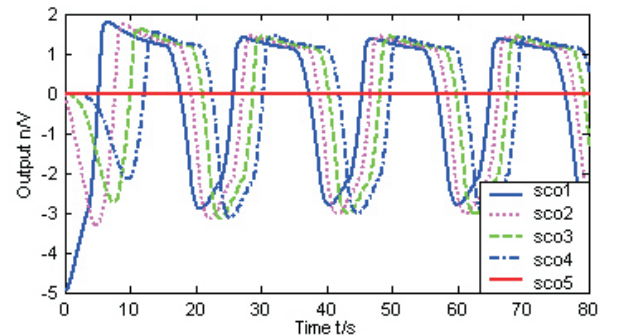


Fig. 10. CPGs' output of the CPG network

Fig.10 and the initial condition in section VI.2 as the input to the dynamic simulation model. The corresponding locomotion was achieved, as shown in the Fig.11, Fig.12 and Fig.13.



Fig. 11. Serpentine locomotion pattern



Fig. 12. Concertina locomotion pattern



Fig. 13. Side wind locomotion pattern

3) *Experiments*: Some experiments were carried out on “Perambulator” to testify the validity of the proposed CPG control architecture. The robot moved on the smooth floor. Using the initial high level command of [100], [010], [001] to fire  $[n_y, n_p, n_m]$  of first CPG, other CPG were unfired at the beginning in the CPG network, the rhythm patterns for serpentine locomotion, concertina locomotion and side winding locomotion were achieved. The corresponding experiment results were shown in Fig.14, Fig.15 and Fig.16.

Because the parameters in simulation model and real snake-like robot can not be the same, the results of them are not well according with each other. But they showed the same trend in shape and locomotion as we expected.

## VII. CONCLUSIONS

It is very hard to explain the mechanism of a genuine biological characteristic of the locomotion in living snakes just with simple method. In the present paper, we designed an artificial CPG without a feedback control loop. Our control system was based on the CPG model constructed from the bidirectional cyclic inhibitory neural oscillator. In order to achieve stable locomotion, we investigated the stability of the bidirectional cyclic inhibitory CPG. Moreover, a numerical condition for it to sustain a rhythm was presented for the first time. The dynamics simulations and experiment were carried out to verify the validity of generation of the different locomotion rhythmic pattern by the CPG just with different high level command. Both the simulation and experiment results have shown that the CPG control system can well

imitate the mechanism of the rhythmic pattern generation as we found in living snakes.

In the future study, we will specify the function of the feedback in the bidirectional cyclic inhibitory CPG to achieve a more efficient locomotion of the snake-like robot in different terrains.



Fig. 14. Serpentine locomotion



Fig. 15. Concertina locomotion



Fig. 16. Side wind locomotion

## REFERENCES

- [1] Bauchot R., Snakes-a nature history. Sterling Publishing Company, Inc. New York, 1994:60-75.
- [2] Frasca M., Arena P. Fortuna L., Bio-Inspired Emergent Control of Locomotion System. World Series A.2004, Vol.48.
- [3] Harmon L., Lewis E., Neural modeling. Physical Review, 1966, 46(5): 513-591.
- [4] Reisis R., A theory and simulation of rhythmic behavior due to reciprocal inhibition in nerve nets. Proc. of the 1963 A.F.I.P.S. Spring Joint Computer Conference. Vol.21 National Press, pp. 171-194.
- [5] Kling U., Szekely G., Simulation of rhythmic nervous activities. I. Function of networks with cyclic inhibitions. Kybernetik. Vol (5), pp. 89-103.
- [6] Matsuoka K., Sustained oscillations generated by mutually inhibiting neurons with adaptation. Biological Cybernetics, 1985, 52(5):367-376.
- [7] Hirose S., Biologically Inspired Robots (Snake-like Locomotor and Manipulator), Oxford University Press, 1993.
- [8] Inoue K., Ma S., Jin C., Neural oscillator network-based controller for meandering locomotion of snake-like robots. Proc. 2004 IEEE Int. Conf. on Robotics and Automation (ICRA'04), 4.2004:5064-5069.
- [9] Lu Z., Ma S., Li B., Wang Y., 3D locomotion of a snake-like robot controlled by cyclic inhibitory CPG model. Proc. 2006 IEEE Int. Conf. on Intelligent Robotics and System (IROS'06),10,2006(in press).
- [10] Lu Z., Ma S., Li B., Wang Y., Serpentine locomotion of a snake-like robot controlled by cyclic inhibitory CPG model. Proc. 2005 IEEE Int. Conf. on Intelligent Robotics and System (IROS'05),8,2005: 3019-3024
- [11] Lu Z., Ma S., Li B., Wang Y., Design of a snake-like robot controller with cyclic inhibitory CPG model. Proc. 2005 IEEE International Conference on Robotics and Biomimetics (ROBIO'05),7,2005: 35-40.
- [12] Gray J., “The mechanism of locomotion in snake,” Exp. Bio.23. 1946, pp. 101-120.
- [13] Shepherd G. M., Neurobiology. Oxford Univ. Press.
- [14] Matsuoka K., Mechanisms of frequency and pattern control in the neural rhythm generators. Biological Cybernetics, 1987, 56(5):345-353.